Science Press

ARTICLE

Effect of Pr Addition on Microstructure, Phase Transformation Behavior, and Hardness of Ni-Rich NiTi Shape Memory Alloy

Zhao Shilei,   Zhao Kun,   Wang Fuwen

Baotou Medical College, Baotou 014040, China

Abstract: The influence of Pr addition on the microstructure, phase transformation, and hardness of $Ni_{50}Ti_{50-x}Pr_x$ (x=0, 0.1, 0.3, 0.5, 0.7, 0.9, at%) shape memory alloys was investigated. Results show that $Ni_{50}Ti_{50-x}Pr_x$ alloys consist of NiTi matrix and NiPr precipitates. $Ni_{50}Ti_{49.5}Pr_{0.5}$ alloy has the optimal properties of martensitic transformation start temperature of 73 °C, the thermal hysteresis as narrow as 37 °C, and the Vickers hardness of 2850 MPa. Pr addition obviously decreases the martensitic transformation temperature of NiTi alloys, but the composite alloy maintains a relatively narrow thermal hysteresis and relatively high Vickers hardness, compared with other NiTi-based shape memory alloys.

Key words: NiTiPr; microstructure; phase transformation; hardness

NiTi-based shape memory alloys (SMAs) have unique shape memory effects and superelasticity behavior, which have been applied in various fields, especially in engineering and medical applications[1]. Current researches about SMAs mainly focus on controlling the transformation temperatures and improving the shape memory effect. The phase transformation behavior of NiTi-based SMAs is strongly dependent on composition, alloying, precipitates, and heat treatment history[2]. Experimental researches suggest that the influence factors of phase transformation temperature are the elastic properties of the parent austenite and certain microstructural features, such as precipitates[3]. Alloying is a frequently used approach for tuning the transformation temperatures of NiTi-based SMAs. Alloying elements change not only the transformation temperatures but also the transformation product and the transformation route of NiTi-based SMAs[4]. To date, transition metals such as Fe[5], Cu[6], Nb[7], Ta[8], Zr[9], Hf[10], Au[11], and Pd[12] have been adopted as alloying elements for NiTi-based SMAs, and their influences on microstructure, phase transformation, and mechanical properties have been comprehensively studied. It is found that most transition metals lower the transformation temperatures, but some transition metals, such as Zr, Hf, Au, and Pd, increase the

transformation temperatures by 100 °C[9]. Therefore, NiTiZr, NiTiHf, NiTiAu, and NiTiPd are considered as candidates for high temperature SMAs[2]. However, Au and Pd are noble metals, indicating that the large-scale applications of NiTiAu and NiTiPd are restricted because of their high cost. Considering the high transformation temperatures and low cost, NiTiHf SMA is a favorable candidate of high temperature SMAs for engineering applications[13]. However, NiTiHf SMAs always exhibit a wide thermal hysteresis (>50 °C), which is not beneficial to fast actuation applications (such as Micro-electronmechanical system and robotics) [13,14]. Thus, quaternary NiTi-based SMAs such as NiTiHfTa[15] are designed for improving the functional properties through microstructural modifications. However, the thermal hysteresis of $Ni_{49}Ti_{36}Hf_{15-x}Ta_x$ (x=0, 3, 6, 9, 12, at%) SMAs is still wide, ranging from 50.0 °C to 80.8 °C.

Rare earth (RE) elements are often added into various alloys to tune their properties. The influence of RE elements (such as Ce[16], Gd[17], Dy[18], Nd[19], and La[20]) addition on the microstructure and phase transformation behavior of binary NiTi SMAs has also been studied. The addition of Ce, Gd, and Dy into NiTi alloy can increase the transformation temperature because some new type second precipitates exist

in the TiNiRE SMAs, changing the Ni/Ti ratio of the matrix[21]. Recently, the influence of RE elements addition on microstructure, phase transformation, and mechanical properties of TiNiHfY SMAs has been systematically investigated[22]. It is found that the Y addition slightly decreases the transformation temperature, whereas the thermal hysteresis is still wide and almost keeps constant at ~50 °C as the Y content changes. Pr is another widely applied RE element, especially in the use of magnetic materials. However, few studies have been conducted on the addition of Pr into NiTi SMA. Therefore, the influence of Pr addition on microstructure, phase transformation, and mechanical properties of TiNiPr SMAs remains unclear.

In this research, NiTiPr SMAs with Pr content of 0.1at%~0.9at% were prepared via arc-melting, and the microstructure, phase transformation behavior, and hardness were studied.

1 Experiment

The NiTiPr alloys were prepared by melting raw materials of Ti (purity 99.9wt%), Ni (purity 99.7wt%), and Pr (purity 99.95wt%) with different nominal composition in a vacuum non-consumable arc-melting furnace using a water-cooled copper crucible. The $Ni_{50}Ti_{50-x}Pr_x$ alloys with x=0, 0.1, 0.3, 0.5, 0.7, 0.9 are $Ni_{50}Ti_{50}$, $Ni_{50}Ti_{49.9}Pr_{0.1}$, $Ni_{50}Ti_{49.7}Pr_{0.3}$, $Ni_{50}Ti_{49.5}Pr_{0.5}$, $Ni_{50}Ti_{49.3}Pr_{0.7}$, $Ni_{50}Ti_{49.1}Pr_{0.9}$ alloys in atom percentage, respectively. Arc-melting was conducted for four times to ensure the uniformity of composite. The as-prepared alloys were spark-cut from the ingots and solution-treated at 850 °C for 1 h in a vacuum quartz tube furnace. Subsequently, the alloys were quenched with water. Thereafter, the specimens were mechanically and lightly polished to obtain a plain surface for the observation of microstructure and phase transformation behavior.

The morphology of $Ni_{50}Ti_{50-x}Pr_x$ alloys was observed using scanning electron microscope (SEM, TM3030, Hitachi, Tokyo, Japan) equipped with energy dispersive spectrometer (EDS, Oxford). X-ray diffraction (XRD) patterns were obtained using a D/MAX-2500PC X-ray diffractometer (Rigaku, Tokyo, Japan). The phase transformation temperatures of the $Ni_{50}Ti_{50-x}Pr_x$ alloys were measured by differential scanning calorimeter (DSC, Q2000, TA Instrument, New Castle, USA) with a scanning range of 0~550 °C and a scanning rate of 10 °C/min during heating and cooling procedure. The microstructure was in-situ observed under a transmission electron microscope (TEM, JEM-2010, JEOL Ltd., Tokyo, Japan) at 200 kV. TEM images were recorded with a Gatan 1 k×1 k CCD and processed using the DigitalMicrograph software. The hardness of $Ni_{50}Ti_{50-x}Pr_x$ and NiTi SMAs were measured using a HXD-1000TMC/LCD Vickers hardness tester.

2 Results and Discussion

Fig.1 depicts SEM back-scattered electron (BSE) images of all six alloys. For NiTi alloy without Pr, the morphology is uniform and featureless (Fig.1a). For $Ni_{50}Ti_{50-x}Pr_x$ alloys with x =0.1, 0.3, 0.5, 0.7, 0.9, white particles and gray matrixes can be identified in Fig.1b~1f, and the number of the particles shows an evident increase with the increase in Pr content. The chemical composition of $Ni_{50}Ti_{50-x}Pr_x$ alloys was analyzed by EDS and summarized in Table 1. The Ni:Ti ratio in the matrix of each alloy is very close to 1. Thus, the matrix may be a NiTi binary alloy[23]. According to the isothermal section of ternary alloy phase diagram of $Ni_{50}Ti_{50-x}Pr_x$ alloys at 773 K, no intermetallic compounds can be found in the TiPr binary alloy

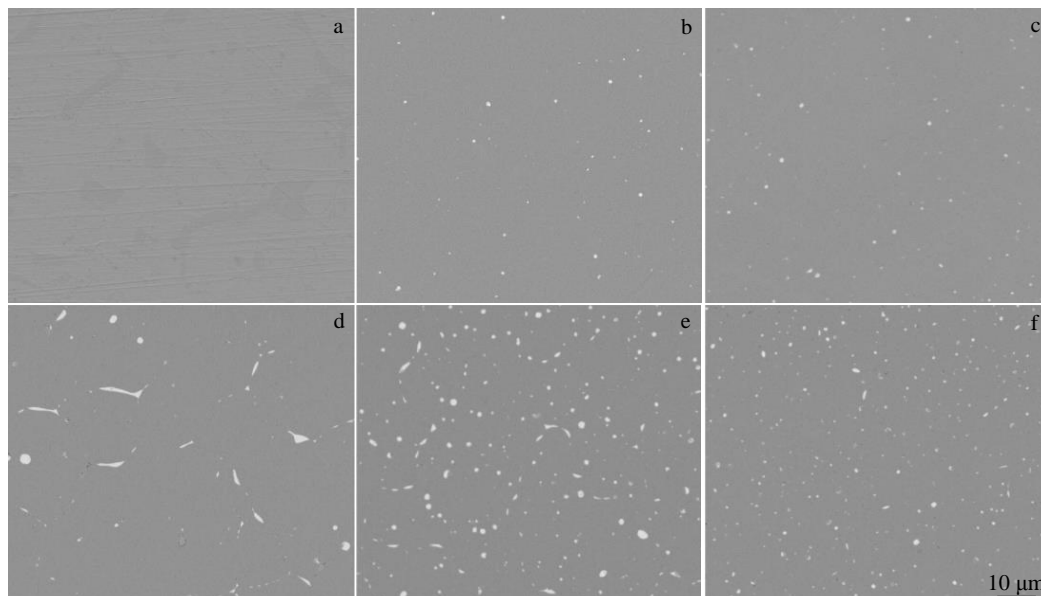Fig.1   SEM-BSE images of $Ni_{50}Ti_{50-x}Pr_x$ alloys: (a) $Ni_{50}Ti_{50}$, (b) $Ni_{50}Ti_{49.9}Pr_{0.1}$, (c) $Ni_{50}Ti_{49.7}Pr_{0.3}$, (d) $Ni_{50}Ti_{49.5}Pr_{0.5}$, (e) $Ni_{50}Ti_{49.3}Pr_{0.7}$, and (f) $Ni_{50}Ti_{49.1}Pr_{0.9}$

Table 1 Chemical composition of $Ni_{50}Ti_{50-x}Pr_x$ SMAs (at%)

x	Component	Ti	Ni	Pr
0	Matrix	49.5	50.5	-
0.1	Matrix	49.7	50.3	0.0
	Precipitate	11.2	48.5	40.3
0.3	Matrix	49.1	50.9	0.0
	Precipitate	11.9	48.2	39.9
0.5	Matrix	49.1	50.9	0.0
	Precipitate	10.8	48.7	40.5
0.7	Matrix	49.4	50.6	0.0
	Precipitate	12.5	48.2	39.3
0.9	Matrix	49.7	50.3	0.0
	Precipitate	12.6	48.2	39.2
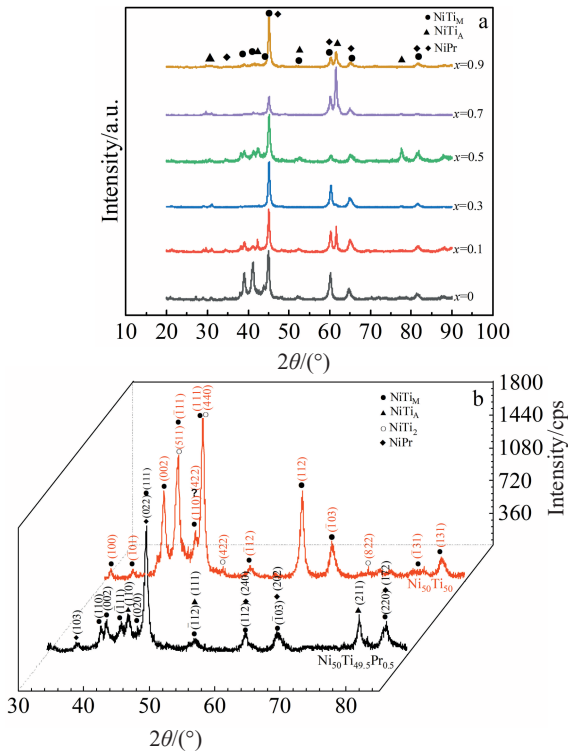
Fig.2   XRD patterns of $Ni_{50}Ti_{50-x}Pr_x$ alloys: (a) $2\theta=10°\sim100°$; (b) $2\theta= 30°\sim85°$

system[24]. Furthermore, the phase diagram shows 7 kinds of intermetallic compounds: PrNi, Pr_3Ni, Pr_7Ni_3, $PrNi_2$, $PrNi_3$, Pr_2Ni_7, and $PrNi_5$[24]. The EDS results show that the Ni:Pr:Ti ratio in the white particles is approximately 48:40:12 and they may be NiPr precipitate with Ti solute.

Fig. 2a depicts the XRD patterns of $Ni_{50}Ti_{50-x}Pr_x$ alloys with $x=0$, 0.1, 0.3, 0.5, 0.7, 0.9 at room temperature. The diffraction peaks are identified as NiTi B19′ martensite, NiTi B2 austenite, $NiTi_2$, NiTi, and NiPr after comparison with JCPDF cards of No.65-0145, No.65-4572, No.72-0442, No.65-2038, and No.19-0837, respectively. The detailed crystal plane indices of $Ni_{50}Ti_{50}$ and $Ni_{50}Ti_{49.5}Pr_{0.5}$ at room temperature are presented in Fig. 2b. The relative intensity of XRD curves

markedly varies owing to the fraction difference of martensite and austenite phases. The letter M and A in Fig.2a denotes the NiTi B19′ martensite and NiTi B2 austenite, respectively. Thus, it can be confirmed that the matrix in $Ni_{50}Ti_{50-x}Pr_x$ alloys is near-equiatomic NiTi binary alloy, whereas the white particles in $Ni_{50}Ti_{50-x}Pr_x$ alloys are NiPr precipitate with Ti solute. This microstructure is highly similar to that of NiTiCe[16], NiTiGd[17], NiTiDy[18], NiTiY[25], and NiTiNd[19].

Fig.3 depicts the DSC curves of $Ni_{50}Ti_{50-x}Pr_x$ alloys and NiTi SMAs. Each DSC curve shows only one peak during the cooling process, which indicates a one-step B2↔B19′ phase transformation[14]. DSC curves of $Ni_{50}Ti_{50-x}Pr_x$ alloys with $x= 0.3$, 0.5, 0.7, 0.9 show two peaks during the heating process, which indicate a two-step B19′→R→B2 transformation. According to the DSC curves, the martensitic transformation start temperature M_s, martensitic transformation peak temperature M_p, and austenite transformation peak temperature A_p are obtained and summarized in Table 2. The M_s of $Ni_{50}Ti_{49.9}Pr_{0.1}$ alloy reaches to 77 °C, which is the highest M_s of the $Ni_{50}Ti_{50-x}Pr_x$ alloys and NiTi SMAs. Meanwhile, with the increase of Pr content, the R→B2 transformation separates from B19′→R transformation, which is similar to the result of Ni_4Ti_3 precipitate in the NiTi binary alloy. Therefore, the NiPr precipitate introduces an extra transformation step and results in a two-step phase transformation. For NiTi-based alloys, the addition of a third element often changes the transformation temperature, transformation product, or the transformation route[2] $Ni_{50}Ti_{49.5}Pr_{0.5}$ alloy has a M_s of 73 °C, and a thermal hysteresis of 37 °C.

It is well known that the M_s of NiTi binary SMA is strongly dependent on Ni content[2]. Ni content increases by about 0.1at% resulting in the decrease of M_s of NiTi binary SMAs by more than 10 °C when Ni content is higher than 50at%[27]. As shown in Table 2, the M_s of $Ni_{50}Ti_{50}$ SMA is 77 °C, whereas the M_s of $Ni_{50.3}Ti_{49.7}$ SMA decreases to 21 °C because of
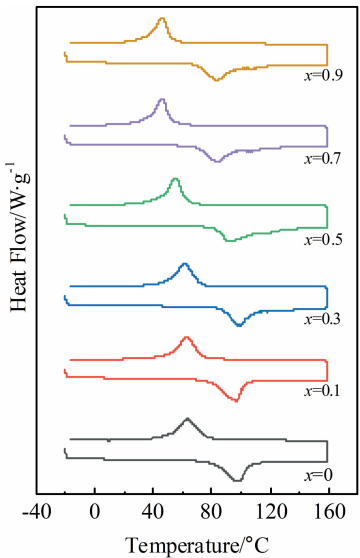

Fig.3   DSC curves of $Ni_{50}Ti_{50-x}Pr_x$ alloys

Table 2　Transformation temperature and hysteresis H_M of different NiTi-based SMAs (°C)

Alloy	M_s	M_p	A_p	H_M	Ref.
$Ni_{50}Ti_{49.9}Pr_{0.1}$	77	63	97	34	-
$Ni_{50}Ti_{49.7}Pr_{0.3}$	74	63	97	34	-
$Ni_{50}Ti_{49.5}Pr_{0.5}$	73	61	98	37	-
$Ni_{50}Ti_{49.3}Pr_{0.7}$	63	54	92	38	-
$Ni_{50}Ti_{49.1}Pr_{0.9}$	53	46	84	38	-
$Ni_{50}Ti_{50}$	77	67	99	32	-
$Ni_{50.3}Ti_{49.7}$	21	10	48	38	[26]
$Ni_{50.45}Ti_{49.05}Ce_{0.5}$	26	20	60	40	[16]
$Ni_{50.7}Ti_{49.3}Gd_1$	65	25	60	35	[17]
$Ni_{50.2}Ti_{48.8}Dy_1$	40	24	62	38	[18]
$Ni_{50.2}Ti_{48.8}Y_1$	36	25	55	30	[25]
$Ni_{50}Ti_{49.5}La_{0.5}$	57	40	80	40	[20]
$Ni_{50}Ti_{48}W_2$	-37	-	-	39	[4]
$Ni_{50}Ti_{45}Ta_5$	44	-	-	53	[4]

the decrease in Ni content. The martensitic transformation finish temperature M_f in all $Ni_{50}Ti_{50-x}Pr_x$ alloys is lower than the room temperature (25 °C). Thus, the martensite transformation cannot completely finish at room temperature, and both NiTi B19′ martensite and NiTi B2 austenite exist in the matrix of $Ni_{50}Ti_{50-x}Pr_x$ alloys. These findings are in agreement with the XRD results. Although the actual Ni content of $Ni_{50}Ti_{50-x}Pr_x$ alloys has a slight difference, the M_s is not notably affected by Ni content, and drops steeply when Ni content increases above the equiatomic content (50at%) [13]. The Ni contents in the matrix of $Ni_{50}Ti_{50-x}Pr_x$ alloys are very close to each other and not higher than 50at% . Therefore, the Ni content is not the main reason for the decrease of M_s of $Ni_{50}Ti_{50-x}Pr_x$ alloys. The martensitic transformation as a coordinated atom movement related to the distance to the habit plane occurs at the crystalline state. Energy accommodated around vacancies, dislocation, and precipitate decreases driving force of the martensitic transformation. The stress generated in these zones requires additional energy for triggering the occurrence of martensitic transformation. In consequence, further overcooling is required for continues transformation. Therefore, the M_s decreases to lower temperature region. It is also well known that the precipitate such as Ni_4Ti_3 in binary NiTi SMA significantly influences the M_s due to the stress state and the Ni depletion in the matrix around the precipitates[2]. In this work, the NiTi matrix and NiPr precipitates form during the preparation process. After heat treatment, the chemical composition of the matrix and precipitates should be uniform; meanwhile the size and quantity of the NiPr precipitates increase with the increase of Pr content. Therefore, the stress around NiPr precipitates is responsible for the decrease of M_s with the increase of Pr content in $Ni_{50}Ti_{50-x}Pr_x$ alloys. A better crystallographic compatibility and a narrow thermal hysteresis are obtained for the $Ni_{50}Ti_{50-x}Pr_x$ alloys, compared to other NiTi-based alloys[28].

Fig. 4 depicts the TEM bright-field (BF) images and selected area electron diffraction (SAED) patterns of martensitic transformation of the $Ni_{50}Ti_{49.5}Pr_{0.5}$ alloy. At room temperature, two different morphologies are identified in the TEM images (Fig. 4a). According to the related SAED and XRD patterns, the observed area in Fig. 4a comprises two phases: the austenite (A) located at the upper left side and the martensite (M) with strip area, which shows the process of martensitic transformation of $Ni_{50}Ti_{49.5}Pr_{0.5}$ alloy clearly. With increasing
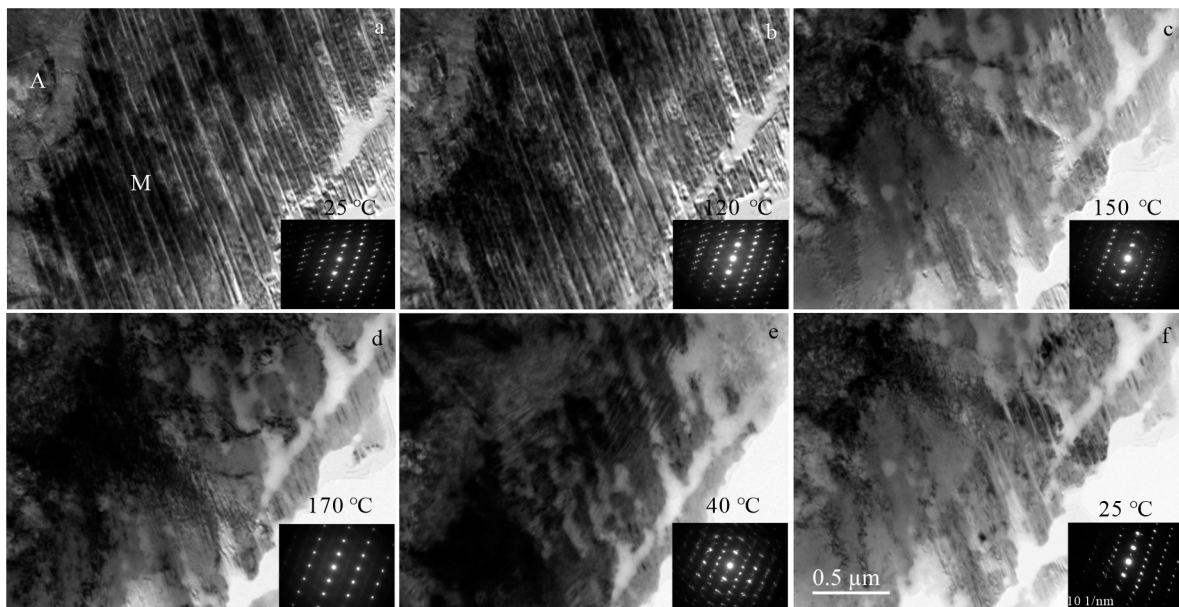

Fig.4　TEM BF images and SAED patterns of martensitic transformation (a~d) and reverse transformation (e, f) of $Ni_{50}Ti_{49.5}Pr_{0.5}$ alloy at 25 °C (a), 120 °C (b), 150 °C (c), 170 °C (d), 40 °C (e), and 25 °C (f)

the temperature, the martensite changes to austenite. However, during the cooling process, the austenite changes to martensite again, which is verified by the EDS and XRD results.

Fig. 5 depicts the XRD patterns of $Ni_{50}Ti_{49.5}Pr_{0.5}$ alloy at 25 and 150 °C. The diffraction peaks are identified as the NiTi B19′ martensite and NiTi B2 austenite after comparison with JCPDF cards of No.65-0145 and No.65-4572, respectively. At 25 °C, the $Ni_{50}Ti_{49.5}Pr_{0.5}$ alloy contains NiTi B19′ martensite, NiTi B2 austenite, and NiPr precipitate, whereas at 150 °C, the $Ni_{50}Ti_{49.5}Pr_{0.5}$ alloy contains NiTi B2 austenite and NiPr precipitate, which is in agreement with the in-situ TEM observation (Fig.4).

Hardness is closely related to the material yield strength and has been regarded as an indicative parameter of mechanical properties of NiTi-based SMAs[14,22,26,29,30]. Thus, the hardness value of $Ni_{50}Ti_{50-x}Pr_x$ alloys was measured, as shown in Fig. 6. The hardness value of $Ni_{50}Ti_{49.5}Pr_{0.5}$ alloy is 2850 MPa, which is larger than that of binary $Ni_{50}Ti_{50}$ SMA. This can be explained by the solid solution strengthening effect. The bigger Pr atoms and substitution of Pr for Ti in $Ni_{50}Ti_{50-x}Pr_x$ alloys lead to the linear increase in alloy hardness[31]. Compared with that of $Ni_{50}Ti_{49.5}Pr_{0.5}$ alloy, the hardness of $Ni_{50}Ti_{49.3}Pr_{0.7}$ and $Ni_{50}Ti_{49.1}Pr_{0.9}$ decreases by 200 (7%,) and 300 MPa (10.5%,), respectively. Previous reports

demonstrate that the hardness of NiTi-based SMAs can be influenced by precipitates[14], thermal treatment[30], and quaternary alloying[22], as shown in Table 2. SEM-BSE observation (Fig. 1) confirms that the size of NiPr precipitates increases with the increase of Pr content in $Ni_{50}Ti_{50-x}Pr_x$ alloy. Consequently, the yield strength decreases with the increase of Pr content in $Ni_{50}Ti_{50-x}Pr_x$ alloys[14]. The decline in hardness of $Ni_{50}Ti_{50-x}Pr_x$ alloys can be explained by the Orowan mechanism[30]. The martensitic transformation start temperature decreases gradually with the increase of Pr content. However, $Ni_{50}Ti_{50-x}Pr_x$ alloys keep a relatively narrow thermal hysteresis and high Vickers hardness, compared with other NiTi-based SMAs.

3 Conclusions

1) The microstructure of $Ni_{50}Ti_{50-x}Pr_x$ alloys consists of the NiTi matrix and NiPr precipitates. The $Ni_{50}Ti_{50-x}Pr_x$ alloys have a two-step phase transformation during heating process and one-step transformation during cooling process.

2) $Ni_{50}Ti_{49.5}Pr_{0.5}$ alloy has a martensitic transformation start temperature of 73 °C, a thermal hysteresis of 37 °C and a Vickers hardness as high as 2850 MPa.

3) The martensitic transformation start temperature decreases gradually with the increase of Pr content. However, $Ni_{50}Ti_{50-x}Pr_x$ alloys keep a relatively narrow thermal hysteresis and high Vickers hardness, compared with other NiTi-based shape memory alloys.

Fig.5   XRD patterns of $Ni_{50}Ti_{49.5}Prf_{0.5}$ alloy at 25 and 150 °C

Fig.6   Hardness of $Ni_{50}Ti_{50-x}Pr_x$ and other NiTi-based alloys

References

1   Otsuka K, Ren X. *Intermetallics*[J], 1999, 7(5): 511

2   Otsuka K, Ren X. *Prog Mater Sci*[J], 2005, 50(5): 511

3   Michutta J, Somsen C, Yawny A *et al*. *Acta Mater*[J], 2006, 54(13): 3525

4   Zarinejad M, Liu Y. *Adv Funct Mater*[J], 2013, 18: 2789

5   Frenzel J, Pfetzing J, Neuking K *et al*. *Mat Sci Eng A*[J], 2008, 481-482: 635

6   Tomozawa M, Kim H Y, Miyazaki S. *Acta Mater*[J], 2009, 57(2): 441

7   Zheng Y F, Zhao L C, Ye H Q. *Mat Sci Eng A*[J], 1999, 273-275: 271

8   Gong C W, Wang Y N, Yang D Z. *Mater Chem Phys*[J], 2006, 96(2-3): 183

9   Bertheville B. *J Alloy Compd*[J], 2009, 398(1-2): 94

10 Meng X L, Cai W, Fu Y D *et al*. *Intermetallics*[J], 2008, 16(5): 698

11 Casalena L, Coughlin D R, Yang F. *Microsc Microanal*[J], 2015, 21(S3): 607

12 Liu Y, Kohl M, Okutsu K *et al*. *Mat Sci Eng A*[J], 2004, 378(1-2): 205

13 Ma J, Karaman I, Noebe D R. *Int Mater Rev*[J], 2010, 55(5): 257

14 Karaca H E, Saghaian S M, Ded G *et al*. *Acta Mater*[J], 2013, 61(19): 7422

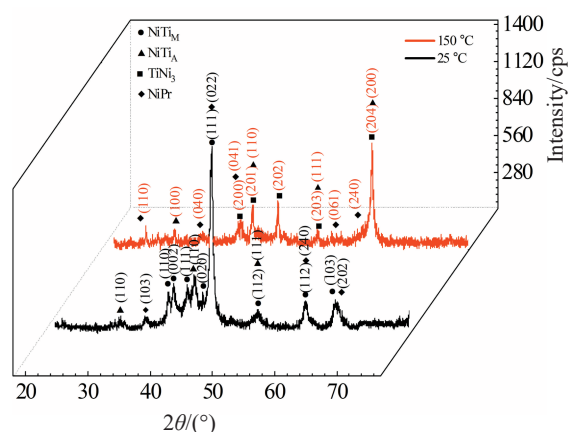15 Prasad R V S, Park C H, Kim S W *et al*. *J Alloy Compd*[J], 2017, 697: 55

16 Cai W, Liu A L, Sui J H *et al. Mater Trans*[J], 2006, 47(3): 716

17 Liu A L, Cai W, Gao Z Y *et al. Mat Sci Eng A*[J], 2006, 438-440: 634

18 Liu A L, Gao Z Y, Gao L *et al. J Alloy Compd*[J], 2007, 437(1-2): 339

19 Dovchinvanching M, Zhao C W, Zhao S L *et al. Adv Mater Sci Eng*[J], 2014, 2014: 489 701

20 Zhao C W, Li W Y, Zhao S L *et al. Vacuum*[J], 2017, 137: 169

21 Cai W, Meng X L, Zhao L C. *Curr Opin Solid St M*[J], 2005, 9(6): 296

22 Yi X Y, Gao W H, Meng X L *et al. Alloy Compd*[J], 2017, 705: 98

23 Itin V I, Bratchikov A D, Merzhanov A G *et al. Combust Explos Shock*[J], 1982, 18(5): 536

24 Zhong X P, Yang Z, Liu J Q. *J Alloy Compd*[J], 2001, 316(1-2): 172

25 Liu A L, Sui J H, Lei Y C *et al. J Mater Sci*[J], 2007, 42(12): 5791

26 Prasher M, Sen D, Tewari R *et al. Mater Chem Phys*[J], 2020, 247: 122 890

27 Frenzel J, George E P, Dlouhy A *et al. Acta Mater*[J], 2010, 58(9): 3444

28 Frenzel J, Wieczorek A, Opahle I *et al. Acta Mater*[J], 2015, 90: 213

29 Yi X, Sun K, Gao W *et al. J Alloy Compd*[J], 2018, 735: 1219

30 Moshref-Javadi M, Seyedein S H, Salehi M T *et al. Acta Mater*[J], 2013, 61(7): 2583

31 Suresh K S, Kim D I, Bhaumik S K *et al. Intermetallics*[J], 2014, 44: 18

富镍镨掺杂镍钛形状记忆合金的微结构、相变特性与硬度

赵石磊，赵　昆，王富文

(包头医学院，内蒙古 包头 014040)

摘　要： 采用真空熔炼法向NiTi二元合金中掺杂Pr稀土元素，制备了多组分原子分数的$Ni_{50}Ti_{50-x}Pr_x$（$x=0$，0.1，0.3，0.5，0.7，0.9）合金。研究了Pr元素的添加对NiTi合金金相组织、相变温度和硬度的影响。结果表明，$Ni_{50}Ti_{50-x}Pr_x$合金由NiTi基体与NiPr夹杂相组成，其中$Ni_{50}Ti_{49.5}Pr_{0.5}$合金的马氏体相变温度达73 ℃，合金的热滞窄至37 ℃，维氏硬度约为2850 MPa。Pr元素的添加显著降低了NiTi合金的马氏体相变温度，同时，与其他NiTi基合金相比，NiTiPr合金保持了较窄的热滞和较高的硬度。

关键词： 镍钛镨；微观结构；相变；硬度

作者简介：赵石磊，男，1988年生，博士，包头医学院，内蒙古 包头 014040，电话：0472-7167815，E-mail：shileizhao@btmc.edu.cn